Journal of Applied Polymer Science

Cellulose Filter Coated with *m*-Aramid for Water Disinfection

Sam Soo Kim,[1] Minji Kim,[1] Jaewoong Lee[2]
[1]Department of Textile Engineering & Technology, Yeungnam University, Gyeongsan, South Korea
[2]Korean Intellectual Property Office, Daejeon, South Korea
Correspondence to: J. Lee (E-mail: leejaew@hotmail.com)

ABSTRACT: Cellulose filters were dipped and padded with *m*-aramid dissolved in *N*,*N*-dimethylacetamide followed by coagulation in distilled water. The coated filters were then chlorinated in a hypochlorite solution. The liquid permeability of the *m*-aramid-coated cellulose filters was examined. The resulting chlorinated and unchlorinated filters were assessed for their ability to disinfect contaminated water. The chlorinated *m*-aramid-coated cellulose filter produced 5 log reductions of *Escherichia coli* and *Staphylococcus aureus*, which was much higher than that observed on the unchlorinated *m*-aramid-coated cellulose filter. © 2013 Wiley Periodicals, Inc. J. Appl. Polym. Sci. 129: 3454–3458, 2013

KEYWORDS: cellulose and other wood products; coatings; separation techniques

Received 15 August 2012; accepted 24 January 2013; published online 28 February 2013
DOI: 10.1002/app.39098

INTRODUCTION

Waterborne diseases are a threat to human health in the third world, where there is a lack of clean water supply, and in the west as a serious complications after heavy rain fall or flooding.[1,2] In addition, international travelers who visit countries with inadequate sanitation facilities or outside water are exposed to waterborne diseases.[3] The presence of waterborne diseases and the development of the drinking water industry have prompted research into water disinfection using materials, such as titanium dioxide photocatalysis[4,5] and silver nanoparticles.[6,7] Titanium dioxide (TiO_2), however, requires light to activate TiO_2 as a photocatalyst. Furthermore, although silver nanoparticles exhibit antimicrobial activity, they may be retained in the drinking water and be observed inside the body. Silver nanoparticles have been reported to damage brain cells, liver cells, stem cells, and the male reproductive system.[8–11]

In terms of separation, nanofiltration (NF) and reverse osmosis (RO) can remove all the bacteria including waterborne pathogens in water and have been used in the drinking water industry. Even though NF and RO can remove bacteria completely, relatively high pressures are needed to perform this separation.[12,13]

On the other hand, there has been increasing demand for affordable and nonpressure driven filtration for water disinfection in the third world, areas lacking sanitation, or some places after heavy rain fall or flooding. A previous study[14] introduced an electro-spun *m*-aramid membrane and a chlorinated membrane to water disinfection via nonpressure driven filtration. Despite the adequate water disinfection, the electro-spun *m*-aramid membrane required electrospinning as a mandatory process, which is a specialized process incurring additional cost, equipment, and steps.

This study fabricated a nonpressure driven filter for water disinfection using a relatively simple and lower-cost process with conventional filter paper and *m*-aramid. To the best of the authors' knowledge, this is the first report of an *m*-aramid-coated cellulose filter to disinfect water for nonpressure driven filtration purposes. The morphology of the cellulose filter was analyzed by scanning electron microscopy (SEM). The mean pore size, pore size distribution, and liquid permeability of the cellulose filters were characterized using a capillary flow porometer. The *m*-aramid coating on the cellulose filter and the subsequent chlorination of the *m*-aramid-coated filters were confirmed by X-ray photoelectron spectroscopy (XPS) and Fourier transform infrared spectroscopy (FTIR). The water disinfection efficacy of the nonpressure driven filter was examined by the filtration of bacterial solutions.

EXPERIMENTAL

Materials

N,*N*-Dimethylacetamide (DMAc) and anhydrous calcium chloride ($CaCl_2$) were obtained from Duksan Pure Chemicals (Ansan, Korea) and used as received. *m*-Aramid was supplied by Yantai Spandex (Yantai, China). Cellulose filters (Grade No. 4 filter paper) with a diameter and thickness of 11 cm and 205 μm, respectively, was purchased from Whatman (Clifton, NJ).

Glass fiber membrane and nylon membrane were Millipore (Bedford, MA) membrane products. The pore size of the glass fiber membrane and nylon membrane were 1 μm and 20 μm, respectively.

Coating of Cellulose Filters with *m*-Aramid

m-Aramid was prewashed with distilled water (~ 60°C), ethanol, and acetone, followed by drying overnight at ambient temperature. Once dried, *m*-aramid solutions (1, 3, and 5 wt %) containing DMAc and $CaCl_2$ were prepared using a previous method.[14] The homogeneous *m*-aramid solution was applied to the cellulose filter using a dip–pad-coagulating process. The process was accomplished by padding the cellulose filter through a homogeneous *m*-aramid solution for 5 min to a wet pickup of approximately 100% followed by coagulation in distilled water at ambient temperature for 60 min. The pressure of the pneumatic mangle (NM-450S, Daiei Kagaku Seiki, Kyoto, Japan) for padding was 2 kgf cm^{-2}. The treated cellulose filters were rinsed with distilled water and air-dried. Two replicates were performed for each sample.

SEM

Before the observations, the above-prepared samples were sputter-coated (E-1030, Hitachi, Tokyo, Japan) with an approximately 20 Å gold layer with an argon purge. Imaging was performed using a Hitachi S-4100 (Japan) SEM at a 15 kV accelerating voltage.

XPS

The samples were prepared as mentioned above and air-dried under ambient conditions to avoid possible airborne contaminants. The elemental composition of the coated surface of the filter paper was measured using a ULVAC-PHI Quantera SXM (Japan) and compared with that of pure filter paper. Monochromatic $Al_{k\alpha}$ radiation was used as the X-ray source. The survey scans were taken using a pass energy of 26 eV. The beam size, beam power, and electron source were 100 μm, 100 W, and 18 kV, respectively.

FTIR

The surface of the pure and coated filter paper was characterized by FTIR (Spectrum 100, PerkinElmer Co., Waltham, MA) in attenuated total reflectance (ATR) mode. Germanium (Ge) ATR crystals were used as the internal reflection elements. The sample paper was held against one side of the Ge crystal. The background spectra were obtained with a Ge crystal and nitrogen gas in the absence of the sample paper. The FTIR spectra were scanned over the wave number range of 700–4000 cm^{-1} for 64 scans with a 2 cm^{-1} resolution.

Chlorination and Titration

A 150 mL solution of commercial bleach, which contained 4% hypochlorite, was diluted with 850 mL of distilled water. The pH of the diluted solution was buffered to 7.5 with acetic acid. The *m*-aramid-coated filter papers were soaked in the solution at ambient temperature for 60 min. The chlorinated samples were rinsed with a large excess of distilled water and dried at 45°C for 2 h to remove any unbonded chlorine. An iodometric titration procedure was used to analyze the oxidative chlorine content using a method reported elsewhere.[14]

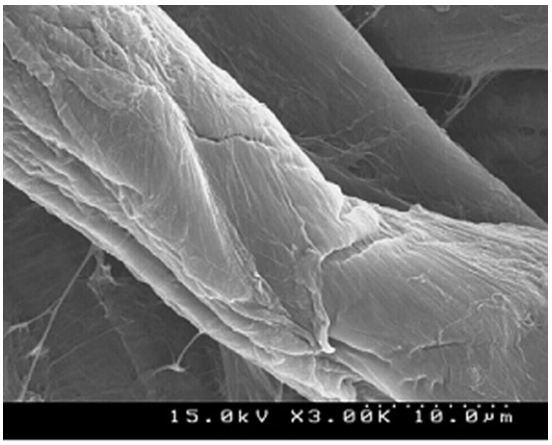

(a)

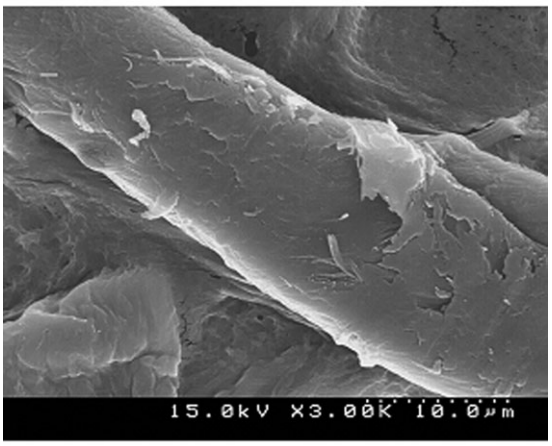

(b)

Figure 1. SEM images of (a) pure filter and (b) 5 wt % *m*-aramid-coated filter.

Capillary Flow Porometry

The liquid permeability of the pure and coated filter paper was determined by capillary flow porometry using a PMI Capillary Flow Porometer (Porous Material Inc., Ithaca, NY). Pure water was used as a working fluid, and the pressure accuracy was 0.15% of the reading.

Water Disinfection Test

Escherichia coli (KCTC 2441) and *Staphylococcus aureus* (KCTC 1621) were incubated in nutrient broth at 37°C for 24 h. The final concentration of *E. coli* (KCTC 2441) and *S. aureus* (KCTC 1621) were 9.16×10^5 and 2.83×10^5 cfu 100 mL^{-1}, respectively. A 100 mL of the bacterial solution was filtered at a flow rate of approximately 100 mL h^{-1}. Two layers of *m*-aramid-coated cellulose filter with a 410 μm thickness were applied. A porcelain Buchner funnel was employed underneath the filters without additional pressure during filtration.

RESULTS AND DISCUSSION

m-Aramid-Coated Filter

The surface of a cellulose filter was treated with a commercially available *N*-halamine precursor, *m*-aramid. Figure 1 shows the SEM images of the *m*-aramid-coated cellulose filter. As

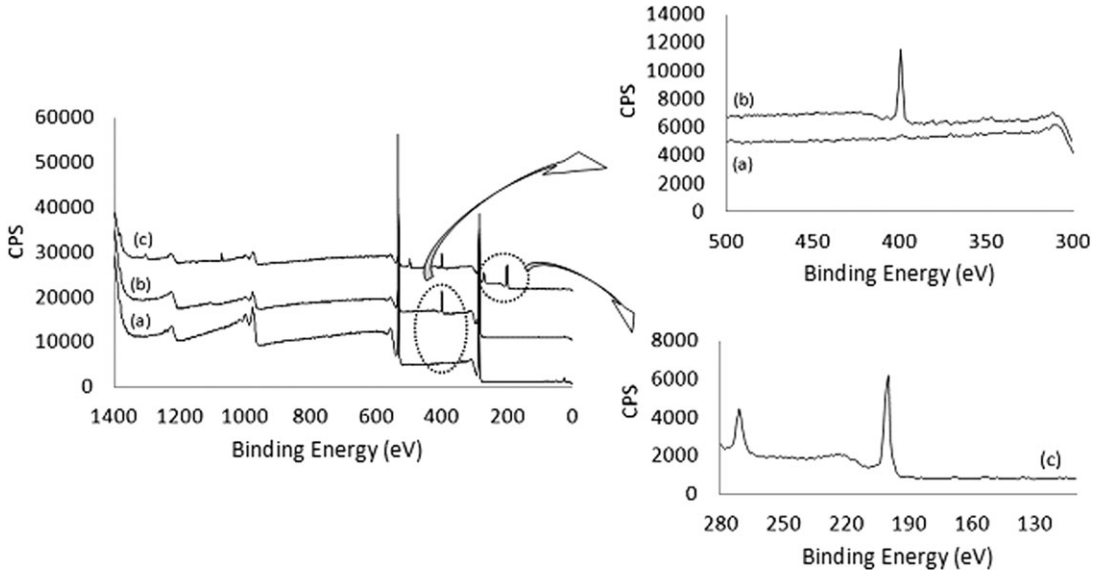

Figure 2. XPS spectra of (a) pure filter and (b) *m*-aramid-coated filter and (c) chlorinated sample of (b).

demonstrated, the pure cellulose filter showed cracks and a rough surface similar to the natural cellulose fiber. On the other hand, the *m*-aramid-coated filter showed a relatively even surface possibly due to the presence of *m*-aramid on the cellulose fiber. A previous study[15] reported that the surface morphology of *m*-aramid films was dependent on the coagulating media. In particular, the *m*-aramid film from the *m*-aramid/DMAc solution in water showed a relatively more even surface than the other films, which were coagulated with different coagulants, such as methanol, ethanol, and propanol. The results in Figure 1 suggest that water is a good coagulating medium for coating cellulose filters with *m*-aramid/DMAc.

The elemental surface composition of the pure cellulose filter and *m*-aramid-coated cellulose filter were measured by XPS (Figure 2). The *m*-aramid-coated filter revealed a distinguishable peak at binding energy of 398.7 eV, which was representative of nitrogen. Since the nitrogen peak was not observed on the cellulose filter, the presence of nitrogen could be used to distinguish *m*-aramid [Figure 2(a)].

The pure cellulose filter showed FTIR bands at approximately 3400 cm^{-1}, 2900 cm^{-1}, and 1420 cm^{-1} (Figure 3), which were assigned to the O–H stretching band, C–H stretching band, and CH_2 bending band, respectively.[16,17] New bands at 1654 cm^{-1} and 1524 cm^{-1} for the coated *m*-aramid onto the filter were considered characteristic of *m*-aramid, which were assigned to the amide I band and bending vibration of N–H, respectively.[18] The observation of a relatively smooth surface in the SEM images, a new peak in the XPS spectra, and new bands in the FTIR spectra confirmed that *m*-aramid had been coated onto the cellulose filter surfaces.

Chlorination of Filters

Regarding the disinfection of bacteria in the contaminated water using an *N*-halamine material, oxidative chlorine is a key source to inactivate bacteria. Thus, the existence and amount of oxidative chlorine on the samples should be considered. FTIR and XPS were used to confirm the chlorination of the sample.

The FTIR spectrum of the *m*-aramid-coated filter (Figure 3) showed a band at 1654 cm^{-1} before chlorination, which is considered to be the amide I band in *m*-aramid. After chlorination, the amide I band shifted to 1673 cm^{-1}. This band shift toward higher wave numbers suggests that the N–H bond in amide groups of *N*-halamine was changed into a N–Cl bond.[19,20]

After chlorination, new peaks in the XPS spectrum of the *m*-aramid-coated filter [Figure 2(c)] at 200 eV and 271 eV were assigned to Cl 2p and Cl 2s, respectively.[21]

Overall, the band shift of the FTIR spectra toward higher wave numbers and the XPS spectra showing new peaks after chlorination compared to those of unchlorinated samples confirmed the chlorination of the coated *m*-aramid on the cellulose fiber.

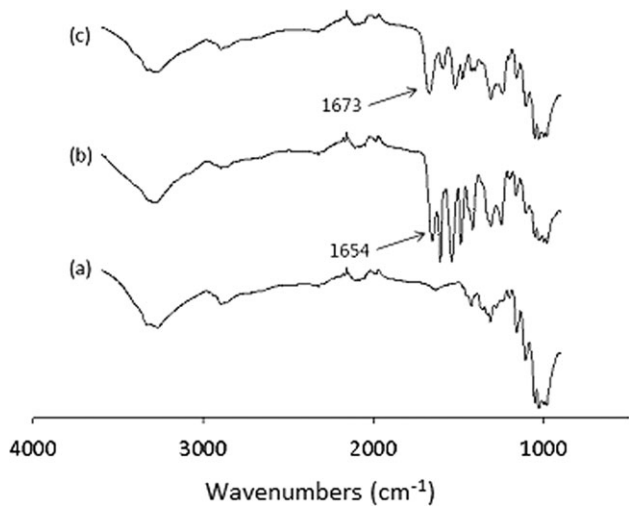

Figure 3. FTIR spectra of (a) pure filter (b) 5 wt % *m*-aramid-coated filter and (c) chlorinated sample of (b).

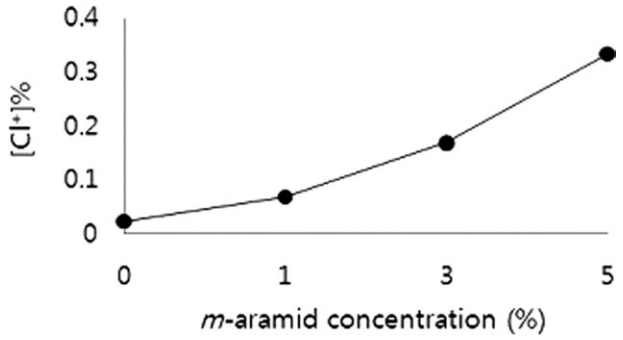

Figure 4. Oxidative chlorine content of 5 wt % *m*-aramid-coated filter.

Figure 4 presents the oxidative chlorine contents of the chlorinated filters. The oxidative chlorine content varied with the concentration of *m*-aramid, i.e., the oxidative chlorine content increased with increasing *m*-aramid concentration in the coating solution.

Filtration Properties of Filters

As observed above, the chlorine content of the filters is dependent on the amount of *m*-aramid on the cellulose filters. On the other hand, the amount of *m*-aramid coated on the cellulose filter should not be too high to prevent its use as a nonpressure driven water filter. Therefore, the permeability of the filters before and after treatment with *m*-aramid was considered.

The pore size distribution of the filters was measured (Figure 5), and the liquid permeability was evaluated to confirm the filtration properties as a nonpressure driven water filter (Figure 6). The pore size of the voids of the filters decreased with increasing *m*-aramid content in the *m*-aramid/DMAc solutions. On the other hand, the pore size distribution of the filters before and after chlorination showed different tendency. More specifically, the pore size of the filters treated with 5 wt % *m*-aramid was increased after chlorination. Thus, the liquid permeability of the filter was also enhanced after chlorination. It is presumed that the unbounded *m*-aramid on the filter might be desorbed from the coating layer during chlorination.

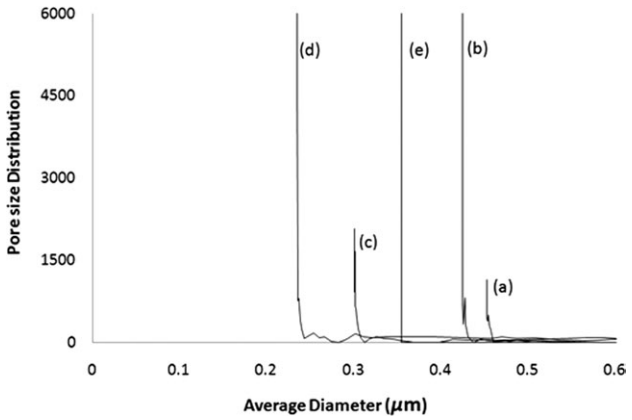

Figure 5. Pore size distribution of (a) pure filter, (b) 1 wt % *m*-aramid-coated filter, (c) 3 wt % *m*-aramid-coated filter, (d) 5 wt % *m*-aramid-coated filter, and (e) chlorinated sample of (d).

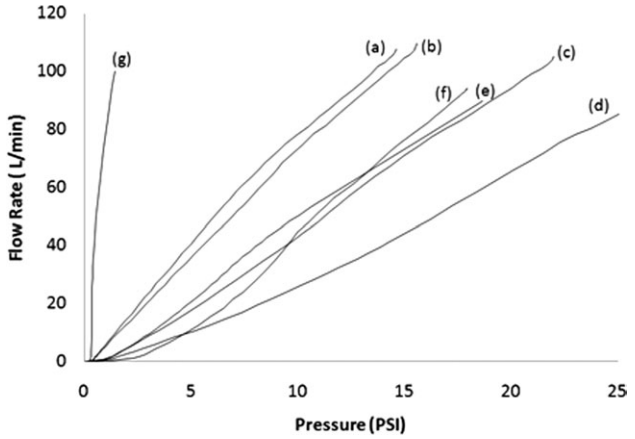

Figure 6. Liquid permeability of (a) pure filter, (b) 1 wt % *m*-aramid-coated filter, (c) 3 wt % *m*-aramid-coated filter, (d) 5 wt % *m*-aramid-coated filter, (e) chlorinated sample of (d), (f) glass fiber membrane (pore size = 1 μm), and (g) nylon membrane (pore size = 20 μm).

The flow rate of the filters decreased with decreasing pore sizes of the filters, suggesting that smaller sized voids delayed the flow of the bacteria suspension. On the other hand, in terms of filtration, the nonpressure driven filtration property was still retained without difficulty up to 5 wt % *m*-aramid.

Water Disinfection Efficacy

As outlined in the "Introduction" section, the aim of this study was to develop a nonpressure driven cellulose filter for water disinfection. Table I lists the water disinfection properties. The pure cellulose filter exhibited almost no disinfection properties against both bacteria, *E. coli* (Gram-negative bacteria) and *S. aureus* (Gram-positive bacteria). On the other hand, after filtration, the chlorinated *m*-aramid-coated cellulose filter disinfected all the bacteria in the solution with 5 log reductions. Interestingly, the *m*-aramid-coated cellulose filter without chlorination showed 1.41 and 1.42 log bacteria reductions against *E. coli* and *S. aureus*, respectively. The mean pore size of the cellulose filters with/without *m*-aramid coating was diverse (Figure 5). Therefore, the decreased diameter of the voids in the *m*-aramid-coated filters might increase the possibility of bacteria retention in the filter instead of the inactivation of bacteria during filtration.

Table I. Antimicrobial Efficacy Against a Bacterial Solution

Samples	*E. coli*[a] Bacterial no. (cfu mL^{-1})	*S. aureus*[b] Bacterial no. (cfu mL^{-1})
Pure filter	7.30×10^5	2.50×10^5
Unchlorinated	3.53×10^4	1.07×10^4
Chlorinated[c]	0	0

[a]Total bacteria: 9.16×10^5 cfu $sample^{-1}$. [b]Total bacteria: 2.83×10^5 cfu $sample^{-1}$. [c]Chlorine content on the filter: 0.34 [Cl^+]%.

Table II. Oxidative Chlorine Content and Rechargeability of Coated Filters with 5 wt % *m*-Aramid Solution (Unit: $[Cl^+]$%)

	Bacterial solution	
Chlorinated filter	*E. coli*	*S. aureus*
Before filtration	0.34	0.34
After filtration	0.12	0.07
After recharge	0.33	0.32

Oxidative chlorine content was examined before and after inactivation of bacteria to demonstrate reproducibility of the filters and the data shown in Table II. As shown in Table II, the coated filters recovered over 94% of the original content of oxidative chlorine through the recharge process. It is suggested that the coated filters possess sufficient reproducibility with a simple recharge process.

Regarding the stability of chlorine on *m*-aramid, a previous study[22] revealed that chlorine content of *m*-aramid/cellulose composite fibers showed without any serious loss over 100 days. Thus, we assumed that the chlorine on the filters coated with *m*-aramid might have relatively proper stability for practical applications.

The inactivation mechanism of *N*-halamine suggests that oxidative chlorine is transferred to the amino groups in the proteins of the microorganism to inhibit its metabolism.[23] Therefore, most of the oxidative chlorine in the chlorinated filter bonds to the bacteria making the bacteria inactive.

CONCUSIONS

m-Aramid was dissolved in a DMAc/$CaCl_2$ solution and coated on cellulose fibers in filter paper. The pore size of the cellulose filters decreased with the enhanced concentration of *m*-aramid in the treating solution. On the other hand, the ability of non-pressure driven filtration for contaminated water was retained without difficulty up to 5 wt % *m*-aramid in the solution. The *m*-aramid-coated cellulose filter possessed sufficient water disinfection effectiveness against a contaminated solution containing *E. coli* (Gram-negative) and *S. aureus* (Gram-positive) after a simple bleach process. This study showed that with a relatively simple coating process using an *m*-aramid solution, cellulose filter can be employed as a new approach for water disinfection. The flow rate of the filter in this study should be improved for practical applications. Therefore, an altered process for enhanced flow rate would be considered in our further study.

REFERENCES

1. Leclerc, H.; Schwartzbrod, L.; Dei-Cas, E. *Crit. Rev. Microbiol.* **2002**, *28*, 371.
2. Hunter, P. R. J. *Appl. Microbiol.* **2003**, *94*, 37S.
3. Backer, H. *Clin. Infect. Dis.* **2002**, *34*, 355.
4. Fernández, P.; Blanco, J.; Sichel, C.; Malato, S. *Catal. Today* **2005**, *101*, 345.
5. Kuhn, K. P.; Chaberny, I. F.; Massholder, K.; Stickler, M.; Benz, V. W.; Sonntag, H.; Erdinger, L. *Chemosphere* **2003**, *53*, 71.
6. Heidarpour, F.; Karim Ghani, W. A.; Wan, A. B.; Bin Ahmadun, F. R.; Sobri, S.; Zargar, M.; Mozafari, M. R. *Dig. J. Nanomater. Bios.* **2010**, *5*, 797.
7. Jain, P.; Pradeep, T. *Biotechnol. Bioeng.* **2005**, *90*, 59.
8. Hussain, S. M.; Javorina, M. K.; Schrand, A. M.; Duhart, H. M.; Ali, S. F.; Schlager, J. J. *Toxicol. Sci.* **2006**, *92*, 456.
9. Hussain, S. M.; Hess, K. L.; Gearhart, J. M.; Geiss, K. T.; Schlager, J. J. *Toxicol.* In Vitro **2005**, *19*, 975.
10. Braydich-stolle, L.; Hussain, S.; Schlager, J. J.; Hofmann, M. C. *Toxicol. Sci.* **2005**, *88*, 412.
11. Soto, K. F.; Carrasco, A.; Powell, T. G.; Garza, K. M.; Murr, L. E. J. *Nanopart. Res.* **2005**, *7*, 145.
12. Pervov, A. G.; Dudkin, E. V.; Sidorenko, O. A.; Antipov, V. V.; Khakhanov, S. A.; Makarov, R. I. *Desalination* **2000**, *132*, 315.
13. Uyak, V.; Koyuncu, I.; Oktem, I.; Cakmakci, M.; Toroz, I. J. *Hazard. Mater.* **2008**, *152*, 789.
14. Kim, S. S.; Jung, D.; Choi, U. H.; Lee, J. *Ind. Eng. Chem. Res.* **2011**, *50*, 8693.
15. Kim, J.; Jung, J.; Kim, S. S.; Lee, J. J. *Korean Soc. Dyers Finishers* **2009**, *21*, 63.
16. Baiardo, M.; Frisoni, G.; Scandola, M.; Licciardello, A. J. *Appl. Polym. Sci.* **2002**, *83*, 38.
17. Pandey, K. K. J. *Appl. Polym. Sci.* **1999**, *71*, 1969.
18. Sun, Y.; Sun, G. *Ind. Eng. Chem. Res.* **2004**, *43*, 5015.
19. Ren, X.; Kocer, H. B.; Worley, S. D.; Broughton, R. M.; Huang, T. S. *Carbohydr. Polym.* **2009**, *75*, 683.
20. Chen, Y.; Worley, S. D.; Kim, J.; Wei, C. L.; Chen, T. Y.; Suess, J.; Kawai, H.; Williams, J. F. *Ind. Eng. Chem. Res.* **2003**, *42*, 5715.
21. Dickerson, M. B.; Lyon, W.; Gruner, W. E.; Mirau, P. A.; Slocik, J. M.; Naik, R. R. *ACS Appl. Mater. Interfaces* **2012**, *4*, 1724.
22. Lee, J.; Broughton, R. M.; Worley, S. D.; Huang, T. S., *J. Eng. Fiber. Fabr.* **2007**, *2*, 25.
23. Denyer, S. P.; Stewart, G. S. A. *B. Int. Biodeter. Biodegr.* **1998**, *41*, 261.